Human alveolar bone cell proliferation, expression of osteoblastic phenotype, and matrix mineralization on porous titanium produced by powder metallurgy

Rosa, Adalberto Luiz; Crippa, Grasiele Edilaine; de Oliveira, Paulo Tambasco; Taba Jr., Mario; Lefebvre, Louis-Philippe; Beloti, Marcio Mateus

Publisher's version / Version de l'éditeur:
https://doi.org/10.1111/j.1600-0501.2008.01662.x
Clinical Oral Implants Research, 20, 5, pp. 472-481, 2009-02-25

Adalberto Luiz Rosa
Grasiele Edilaine Crippa
Paulo Tambasco de Oliveira
Mario Taba Jr
Louis-Philippe Lefebvre
Marcio Mateus Beloti

Human alveolar bone cell proliferation, expression of osteoblastic phenotype, and matrix mineralization on porous titanium produced by powder metallurgy

Authors' affiliations:
Adalberto Luiz Rosa, Grasiele Edilaine Crippa, Paulo Tambasco de Oliveira, Marcio Mateus Beloti, Cell Culture Laboratory, School of Dentistry of Ribeirao Preto, University of Sao Paulo, Ribeirao Preto, SP, Brazil
Mario Taba Jr, Department of Oral and Maxillofacial Surgery and Periodontology, School of Dentistry of Ribeirao Preto, University of Sao Paulo, Ribeirao Preto, SP, Brazil
Louis-Philippe Lefebvre, National Research Council Canada, Industrial Materials Institute, Boucherville, Canada

Correspondence to:
Marcio Mateus Beloti
Cell Culture Laboratory
School of Dentistry of Ribeirao Preto
University of Sao Paulo
Av do Cafe
s/n, 14040-904 – Ribeirao Preto
SP
Brazil
Tel.: +55 16 3602 4785
Fax: +55 16 3633 0999
e-mail: mmbeloti@usp.br

Date:
Accepted 29 September 2008

To cite this article:
Rosa AL, Crippa GE, De Oliveira PT, Taba M Jr, Lefebvre L-P, Beloti MM. Human alveolar bone cell proliferation, expression of osteoblastic phenotype, and matrix mineralization on porous titanium produced by powder metallurgy.
Clin. Oral Impl. Res. **20**, 2009; 472–481.
doi: 10.1111/j.1600-0501.2008.01662.x

Key words: cell culture, osteoblastic cells, porosity, powder metallurgy, titanium

Abstract

Objective: This study aimed at investigating the influence of the porous titanium (Ti) structure on the osteogenic cell behaviour.

Materials and methods: Porous Ti discs were fabricated by the powder metallurgy process with the pore size typically between 50 and 400 μm and a porosity of 60%. Osteogenic cells obtained from human alveolar bone were cultured until subconfluence and subcultured on dense Ti (control) and porous Ti for periods of up to 17 days.

Results: Cultures grown on porous Ti exhibited increased cell proliferation and total protein content, and lower levels of alkaline phosphatase (ALP) activity than on dense Ti. In general, gene expression of osteoblastic markers–runt-related transcription factor 2, collagen type I, alkaline phosphatase, bone morphogenetic protein-7, and osteocalcin was lower at day 7 and higher at day 17 in cultures grown on porous Ti compared with dense Ti, a finding consistent with the enhanced growth rate for such cultures. The amount of mineralized matrix was greater on porous Ti compared with the dense one.

Conclusion: These results indicate that the porous Ti is an appropriate substrate for osteogenic cell adhesion, proliferation, and production of a mineralized matrix. Because of the three-dimensional environment it provides, porous Ti should be considered an advantageous substrate for promoting desirable implant surface–bone interactions.

Titanium (Ti) is largely used as an implant biomaterial due to its mechanical properties and high *in vitro* and *in vivo* biocompatibility, allowing direct bone-to-implant contact (Brånemark 1983; Klokkevold et al. 1997; Pilliar 1998; Castellani et al. 1999; Puleo & Nanci 1999; Faria et al. 2003; Rosa & Beloti 2003; De Oliveira & Nanci 2004; Liu et al. 2004; Kroese-Deutman et al. 2005; Rosa et al. 2006; Brama et al. 2007; De Oliveira et al. 2007). Over the past 35 years, most Ti implants have been designed in dense forms, varying the surface topography. However, some limitations such as interfacial instability with host tissues, and lack of biological anchorage for tissue ingrowth may be associated with dense Ti implants (Pilliar et al. 1981; Pilliar 1983; Li et al. 2005, 2007). In this context, porous biomaterials with a three-dimensional structure could be an alternative to provide biological anchorage for the bone through the ingrowth of mineralized tissue into the pores (Pilliar et al. 1975; Murray & Semple 1981; Maniatopoulos et al. 1986, 1988a, 1988b). Porous metallic implants have been produced using a variety of processes, including chemical vapour infiltration to deposit tantalum onto vitreous carbon foams, solid freeform fabrication, self-propagating high-temperature synthesis, and powder metallurgy (Bobyn

et al. 1999; Melican et al. 2001; Wen et al. 2002; Assad et al. 2003).

Recently, a novel powder metallurgy process for the fabrication of Ti foams has been developed (Lefebvre & Thomas 2003). This process consists of mixing a Ti powder with a polymeric binder and a foaming agent before a three-step thermal treatment. As the characteristics of the pores (pore size, pore shape, porosity, and interconnecting pore size) have been suggested to affect bone cell responses to the porous implants (St-Pierre et al. 2005; Li et al. 2005, 2007), this fabrication process has the advantage that it allows the adjustment of the pore size within the range required for bone ingrowth, from 50 to 400 μm (St-Pierre et al. 2005). In addition, the binder used has clean decomposition characteristics and leaves no residue after sintering at 1400°C. Finally, previous analyses have demonstrated that the surface is essentially composed of a 5-nm-thick titanium oxide and the additives used do not affect the biocompatibility of the material (St-Pierre et al. 2003; Lefebvre & Baril In press).

The mechanical and biological features of the porous Ti make it a potential candidate for applications such as dental implants. It has been demonstrated that a porous Ti structure supports bone-like tissue formation (Kim et al. 2000; Holtorf et al. 2005; Li et al. 2007). In addition, a porous Ti substrate favours cartilage tissue formation by influencing cell attachment and the extent of cell spreading (Spiteri et al. 2006). Nonetheless, to date, few studies have focused on this porous Ti structure and, indeed, little is known about its potential biologic effects. Considering this, the present study was designed to investigate key parameters of the development of the osteoblastic phenotype in human osteogenic cell cultures grown on a porous Ti structure.

Material and methods

Fabrication of Ti substrates

Porous Ti foams were produced as described previously (Lefebvre & Thomas 2003). A pure Ti powder was dry-mixed with a polyethylene binder and a chemical foaming agent (*p*,*p*′-oxybis[benzenesulfonyl hydrazide]). This powder mixture was poured into a mould and foamed at 210°C in air. The resulting material was then debinded at 450°C in argon and pre-sintered under vacuum at 1000°C. Porous Ti and control dense Ti were then machined to obtain discs 10 mm in diameter and 2 mm in thickness. The discs were washed for 15 min in acetone in an ultrasonic bath (Bandelin Sonorex, Amtrex Technologies Inc., St Laurent, QC, Canada). Finally, the porous specimens were sintered at 1400°C to consolidate the material. All samples were autoclaved at 120°C for 40 min before using in the cell culture experiments.

The topography of the dense Ti surface and the porous Ti structure was examined under scanning electron microscopy (SEM–LEO 440, Leo Electron Microscopy Ltd, Cambridge, UK). The surface roughness of the dense Ti was evaluated using an optical profiler Plμ 2300 (Sensofar-Tech, S.L. Terrassa, Spain). The specific surface area of both Ti groups was evaluated by gas adsorption (BET) using a Micrometrics ASAP 2010 system (Micromeritics Instrument Corporation, Norcross, GA, USA) with krypton as an adsorbate. The proportion of oxygen was evaluated by inert gas fusion, and carbon was measured by combustion analysis using LECO analysers (LECO Corporation, St- Joseph, MI, USA).

Culture of osteogenic cells derived from human alveolar bone

Human alveolar bone fragments (explants) were obtained from a healthy donor, using the research protocols approved by the Committee of Ethics in Research of the School of Dentistry of Ribeirao Preto, University of Sao Paulo. Osteogenic cells were obtained from these explants by enzymatic digestion using type II collagenase (Gibco–Life Technologies, Grand Island, NY, USA) as described previously (Beloti et al. 2006, 2008). These cells were cultured in α-minimum essential medium (Gibco), supplemented with 10% foetal bovine serum (Gibco), 50 μg/ml gentamicin (Gibco), 0.3 μg/ml fungisone (Gibco), 10^{-7} M dexamethasone (Sigma, St Louis, MO, USA), 5 μg/ml ascorbic acid (Gibco), and 7 mM β-glycerophosphate (Sigma). Subconfluent cells in primary culture were harvested after treatment with 1 mM ethylenediamine tetraacetic acid (EDTA) (Gibco) and 0.25% trypsin (Gibco) and subcultured in 24-well culture plates (Falcon, Franklin Lakes, NJ, USA) on dense and porous Ti at a cell density of 2×10^4 cells/sample. Cells were subcultured on polystyrene as a control of the culture conditions. During the culture period, cells were incubated at 37°C in a humidified atmosphere of 5% CO_2 and 95% air; the medium was changed every 3 or 4 days.

Fluorescence labelling

At 1, 7, and 14 days, cells were fixed for 10 min at room temperature using 4% paraformaldehyde in 0.1 M phosphate buffer (PB), pH 7.2. After washing in PB, they were processed for indirect immunofluorescence labelling for localization of fibronectin. In addition, cell adhesion and spreading were morphologically evaluated by direct fluorescence with fluorophore-conjugated probes, as described below. Briefly, cells were permeabilized with 0.5% Triton X-100 in PB for 10 min, followed by blocking with 5% skimmed milk in PB for 30 min. Primary monoclonal antibody to fibronectin (1 : 100, clone IST-3, Sigma) was used, followed by a mixture of Alexa Fluor 594 (red fluorescence)-conjugated goat anti-mouse secondary antibody (1 : 200, Molecular Probes, Eugene, OR, USA) and Alexa Fluor 488 (green fluorescence)-conjugated phalloidin (1 : 200, Molecular Probes), which labels actin cytoskeleton. Replacement of the primary monoclonal antibody with PB was used as control. All antibody incubations were performed in a humidified environment for 60 min at room temperature. Between each incubation step, the samples were washed three times (5 min each) in PB. Before mounting for observation under a microscope, cell nuclei were stained with 300 nM 4′,6-diamidino-2-phenylindole, and dihydrochloride (DAPI, Molecular Probes) for 5 min and samples were briefly washed with dH_2O. Dense and porous Ti samples were mounted face up on glass slides, while a Fisherbrand 12 mm round glass coverslip (Fisher Scientific, Suwanee, GA, USA) was mounted with an antifade kit (Vectashield, Vector Laboratories, Burlingame, CA, USA) on the surface containing cells. The samples were then examined using a fluorescence microscope (Leica, Bensheim, Germany) equipped with a Leica DC 300F digital camera under

epifluorescence. The acquired digital images were processed with ADOBE PHOTOSHOP software.

Culture growth

Culture growth was evaluated at days 3, 7, and 10 by the 3-[4,5-dimethylthiazol-2-yl]-2,5- diphenyl tetrazolium bromide (MTT) assay (Mosmann 1983). Cells were incubated with 100 µl of MTT (5 mg/ml) in PBS at 37°C for 4 h. The medium was then aspirated from the well and 1 ml of acid isopropanol (0.04 N HCl in isopropanol) was added to each well. The plates were then agitated on a plate shaker for 5 min, and 100 µl of this solution was transferred to a 96-well format using opaque-walled transparent-bottomed plates (Fisher Scientific, Pittsburgh, PA). The optical density was read at 570–650 nm on the plate reader (µQuant, Biotek, Winooski, VT, USA), and data were expressed as absorbance. Samples of both dense and porous Ti were incubated in culture medium without cells, assayed, and the absorbance was subtracted from the absorbance of experiments carried out with cells to eliminate any background.

Total protein content

The total protein content was calculated at 7 and 10 days in culture, according to the method described by Lowry et al. (1951). The wells were filled with 2 ml of dH_2O. After 5 cycles of thermal shock (alternating temperature between 15 min at 37°C and 20 min at −20°C), 1 ml of the sample from each well was mixed with 1 ml of Lowry solution (Sigma) and left for 20 min at room temperature. After this, 0.5 ml of phenol reagent of Folin and Ciocalteau (Sigma) was added. This was then left for 30 min at room temperature, after which absorbance was measured using a spectrophotometer (CE3021; Cecil, Cambridge, UK) at 680 nm. The total protein content was expressed as µg protein/ml. Samples of both dense and porous Ti were incubated in culture medium without cells, assayed, and the absorbance was subtracted from the absorbance of experiments carried out with cells to eliminate any background.

Alkaline phosphatase (ALP) activity

ALP activity was assayed as the release of thymolphthalein from thymolphthalein monophosphate using a commercial kit (Labtest Diagnostica SA, MG, Brazil). Aliquots of the same wells used for calculating total protein content were assayed in order to measure ALP activity according to the kit instructions. Briefly, 50 µl of thymolphthalein monophosphate was mixed with 0.5 ml of 0.3 mmol/ml diethamine buffer, pH 10.1, and left for 2 min at 37°C. After this, 50 µl of the lysates from each well were added. This was then left for 10 min at 37°C, after which 2 ml of a solution of 0.09 mmol/ml Na_2CO_3 and 0.25 mmol/ml NaOH was added to allow

Table 1. **Primer sequences, annealing temperature (T.A.), melting temperature (T.M.) and product size for real-time PCR reactions**

Target*	Sense and anti-sense sequences	T.A. (°C)	T.M. (°C)	bp
Runx2	TATGGCACTTCGTCAGGATCC AATAGCGTGCTGCCATTCG	61	83	110
COL	TGACGAGACCAAGAACTG CCATCCAAACCACTGAAACC	61	84	114
ALP	ACGTGGCTAAGAATGTCATC CTGGTAGGCGATGTCCTTA	60	86	475
BMP–7	AATTCTTCCACCCACGCTAC TTGGAAAGATCAAACCGGA	57	79	54
OC	CAAAGGTGCAGCCTTTGTGTC TCACAGTCCGGATTGAGCTCA	62	85	150
β-actin	ATGTTTGAGACCTTCAACA CACGTCAGACTTCATGATGG	56	75	495

*Runx2, runt-related transcription factor 2; COL, collagen type I; ALP, alkaline phosphatase; BMP–7, bone morphogenetic protein–7; OC, osteocalcin.

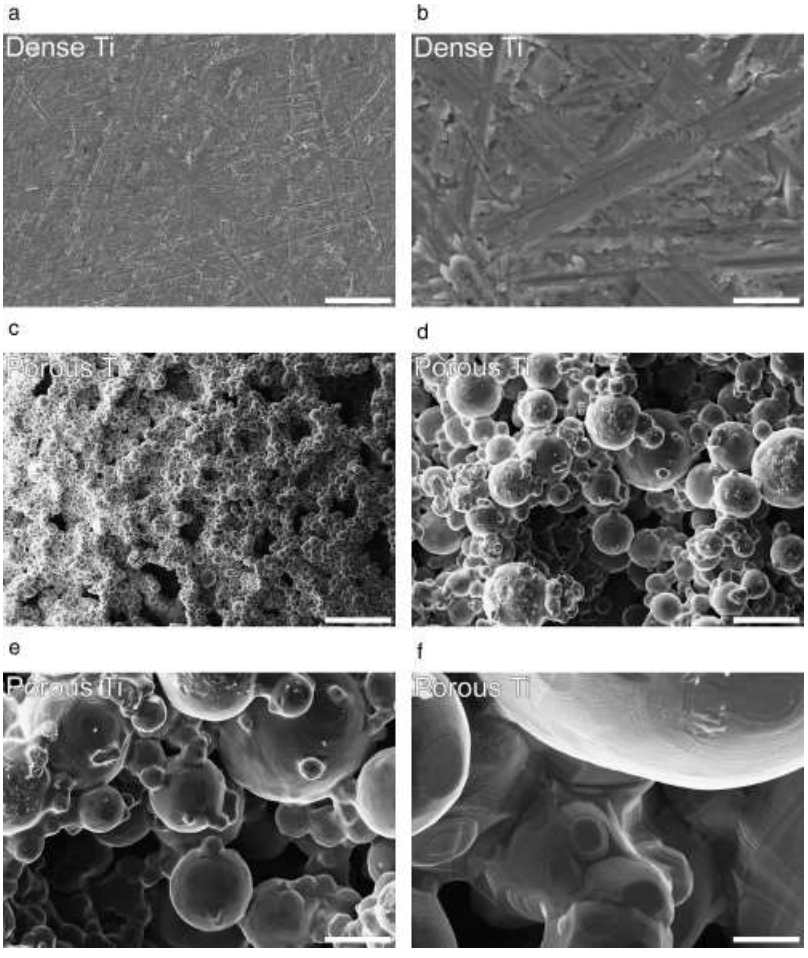

Fig. 1. High resolution scanning electron micrographs of the dense titanium (Ti) and the porous Ti. The dense Ti surface (a and b) showed a slight roughness with many cutting lines. The porous Ti structure (c–f) exhibited a unique topography characterized by a network of spherical particles. At high magnification, porous Ti surface revealed submicron-size steps (f). Scale bars: a and d = 100 µm; b and f = 10 µm; c = 500 µm; e = 50 µm.

colour development to occur. After 30 min, absorbance was measured at 590 nm, results were calculated, and data were expressed as ALP activity normalized by the total protein content measured at 7 and 10 days. Samples of both dense and porous Ti were incubated in culture medium without cells, assayed, and the absorbance was subtracted from the absorbance of experiments carried out with cells to eliminate any background.

RNA extraction and quantitative real-time reverse transcriptase-polymerase chain reaction (real-time PCR)

Gene expressions of runt-related transcription factor 2 (Runx2), collagen type I (COL), ALP, bone morphogenetic protein 7 (BMP–7), and osteocalcin (OC) were evaluated by real-time PCR at days 7 and 17. Gene-specific primers were designed with Primer Express 2.0 (Applied Biosystems, Foster City, CA, USA) and are presented in Table 1.

Total RNA from adherent cells on Ti discs was extracted using the Promega RNA extraction kit (Promega, Madison, WI, USA), according to the manufacturer's instructions. The concentration of RNA was determined by optical density at a wavelength of 260 nm, using the Biomate 3 spectrophotometer (Thermospectronic, Rochester, NY, USA). Complementary DNA (cDNA) was synthesized using 2 μg of RNA through a reverse transcription reaction (M–MLV reverse transcriptase, Promega). Real-time PCR was performed in an ABI Prism 7000 Sequence Detection System using the SybrGreen system (Applied Biosystems, Warrington, UK). SybrGreen PCR MasterMix (Applied Biosystems), specific primers, and 2.5 ng cDNA were used in each reaction. The standard PCR conditions were 95°C (10 min) and 40 cycles of 94°C (1 min), 56°C (1 min), and 72°C (2 min), followed by the standard denaturation curve. For mRNA analysis, the relative level of gene expression was calculated in reference to β-actin expression and normalized by the gene expression of cells subcultured on polystyrene using the cycle threshold (C_t) method (Livak & Schmittgen 2001).

Extracellular matrix formation and mineralization

After culturing for 17 days, the attached cells were fixed with 1.5% glutaraldehyde (Sigma) buffered in 0.1 M sodium cacodylate (Sigma) and dehydrated through a graded series of alcohol. Once dry, the samples were sputter coated with gold and extracellular matrix formations were observed under SEM (LEO).

Matrix mineralization was detected at 17 days by Alizarin Red S (Sigma), which stains areas rich in calcium. Attached cells were fixed in 10% formalin for 2 h at room temperature. After fixation, the specimens were dehydrated through a graded series of alcohol and stained with 2% Alizarin Red S (Sigma), pH 4.2, for 10 min. The samples were then examined by epiluminescence using a fluorescence microscope (excitation filter: 515–560 nm and barrier filter: 590 nm, Leica) equipped with a Leica DC 300F digital camera. The acquired digital images were processed with ADOBE PHOTOSHOP software.

The calcium content was evaluated using a colorimetric method as described

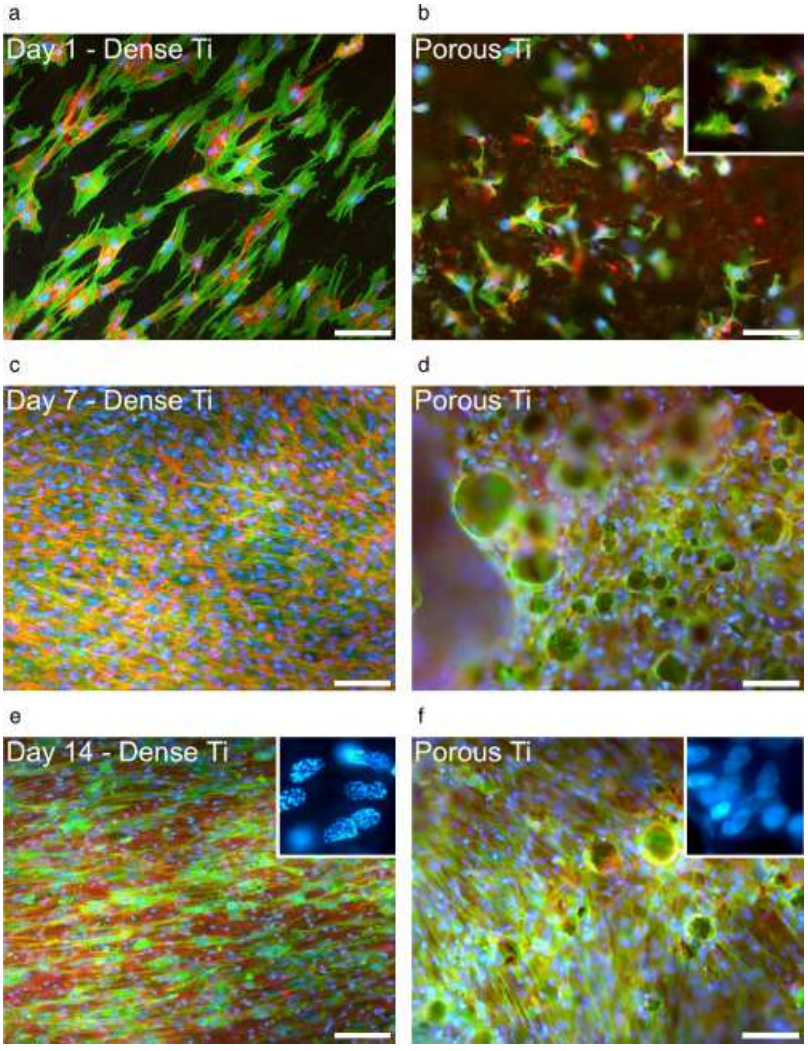

Fig. 2. Fluorescence labelling of osteogenic cells derived from human alveolar bone cultured on dense titanium (Ti) surface (a, c, and e) and porous Ti structure (b, d, and f) at days 1 (a and b), 7 (c and d), and 14 (e and f). Cell-associated green fluorescence reveals actin cytoskeleton (Alexa Fluor 488-conjugated phalloidin). Blue fluorescence indicates cell nuclei (DAPI DNA staining). At 1 day, while cells exhibited an elongated and polyhedral shape on dense Ti surface, the most part of cells cultured on porous Ti structure exhibited a less spread polygonal shape (compare a with b). The spherical characteristic of the porous Ti affected cell morphology during early phases of culture, as a number of cells followed the spheres outline (b inset). At 7 and 14 days, a cell multilayering covering both dense Ti and porous Ti was noticed (c–f) with porous Ti exhibiting a multidirectional cell distribution. Fibronectin labelling (red fluorescence) was observed for cultures grown on dense Ti surface and porous Ti structure at all evaluated time point (a–f). At 1 day, fibronectin was predominantly associated with the cell undersurface (a and b). A different pattern of fibronectin distribution between dense Ti and porous Ti was noticed at days 7 and 14. Cultures grown on dense Ti surface exhibited a higher proportion of apoptotic cells as demonstrated by nuclei stained with DAPI (compare e with f insets). Scale bars: a–f = 50 μm; b, e, and f for insets = 25 μm.

previously (Gregory et al. 2004). Briefly, 280 µl of 10% acetic acid was added to each well containing Ti samples stained with Alizarin Red S, and the plate was incubated at room temperature for 30 min under shaking. This solution was transferred to a microcentrifuge tube and after vortexing for 1 min, the slurry was overlaid with 100 µl of mineral oil (Sigma), heated to exactly 85°C for 10 min, and transferred to ice for 5 min. The slurry was then centrifuged at 20,000 *g* for 15 min and 150 µl of the supernatant was transferred to a new microcentrifuge tube. Then, 60 µl of 10% ammonium hydroxide was added to neutralize the acid and this solution containing 210 µl was read at 405 nm in a 96-well format using opaque-walled transparent-bottomed plates (Fisher Scientific) on the plate reader µQuant (Biotek). Data were expressed as absorbance. Samples of both dense and porous Ti were incubated in culture medium without cells, assayed, and the absorbance was subtracted from the absorbance of experiments carried out with cells to eliminate any background.

Statistical analysis

Experiments of culture growth, total protein content, and ALP activity were carried out in quadruplicate ($n = 4$), gene expression in triplicate ($n = 3$), and calcium content in quintuplicate ($n = 5$). A two-way ANOVA model with interaction between the factors (time period and Ti surface) was used to determine the variability of the parameters culture growth, total protein content, ALP activity, and gene expression. The post hoc Tukey test was used where appropriate. The statistical power was calculated and ranged from 55% to 87%. For calcium content, data were compared by the Mann–Whitney *U*-test. In all the analyses, the level of significance was set at 5%.

Results

Ti substrates

The SEM micrographs of the dense Ti surface and the porous Ti structure are presented in Fig. 1. The dense Ti surface was not perfectly smooth and cutting lines could be observed (Fig. 1a and b), with an average surface roughness of 0.7 µm. The open pores and the spherical aspect were clearly visible in the porous Ti structure (Fig. 1c–f). The porosity of the porous Ti evaluated with the weight and dimensions of the samples was 60% and all the specimens had similar pore sizes, with the pore size distribution within each sample ranging from approximately 50 to 400 µm. The porous Ti presented a higher specific surface area (500 cm^2/g) compared with the dense Ti (2.2 cm^2/g). The dense Ti was mainly composed of Ti with small amounts of oxygen (0.13 wt%) and carbon (0.03 wt%) as impurities. These amounts of oxygen and carbon were lower than that found in the porous Ti structure (0.3 wt% and 0.4 wt%, respectively).

Cell culture experiments

Epifluorescence of actin cytoskeleton labelling at day 1 revealed that adherent cells were spread and randomly distributed throughout the surfaces of both dense and porous Ti (Fig. 2a and b). However, while cells cultured on dense Ti showed an elongated, polyhedral shape (Fig. 2a), the majority of adherent cells on porous Ti presented a less spread polygonal phenotype (Fig. 2b). In addition, cell morphology was affected by the presence of spherical features, as some cells outlined the limits of the largest spheres not covering them at this time point (Fig. 2b inset). As the cultures progressed, at days 7 and 14 both dense Ti and porous Ti exhibited cell multilayering (Fig. 2c–f), with cultures on porous Ti following a multidirectional pattern of cell distribution (Fig. 2d and f). Immunolabelled preparations with an anti-fibronectin antibody revealed that at day 1, all cells promoted fibronectin fibrillogenesis, which was mainly associated with the cell undersurface (Fig. 2a and b). Intense extracellular fibronectin labelling was also observed at days 7 and 14, with a distribution pattern consistent with cell alignment for dense Ti and multidirectional cell growth for porous Ti (Fig. 2c–f). Noticeably, there were more apoptotic cells on dense Ti than on the porous structure, as demonstrated by DAPI nuclear stain (Fig. 2e and f insets).

For the culture growth, two-way ANOVA indicated significant differences regarding Ti surface ($P = 0.0001$), time ($P = 0.0001$), and Ti surface × time interaction ($P = 0.0001$). There were significantly more cells in cultures grown on porous Ti at days 7 ($P = 0.0002$) and 10 ($P = 0.0002$) but not at day 3 ($P = 0.5791$) (Fig. 3 and Table 2). On both dense Ti and porous Ti,

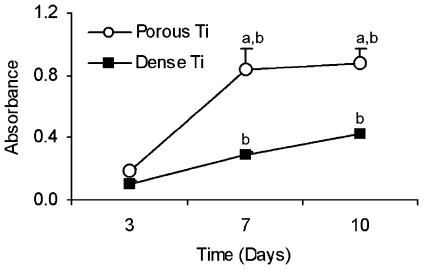

Fig. 3. Growth curves (absorbance) of osteogenic cells derived from human alveolar bone subcultured on dense titanium (Ti) and porous Ti at 3, 7, and 10 days. (a) indicates statistically significant differences ($P \leq 0.05$) between Ti surfaces at each time point. (b) indicates statistically significant differences ($P \leq 0.05$) among 3 and 7 and 10 days. Data are reported as mean ± standard deviation ($n = 4$).

***Table 2*. Quantitative analysis culture growth (absorbance, MTT assay), total protein content (µg/ml), alkaline phosphatase (ALP) activity (µmol thymolphthalein/h/mg protein), and calcium content (absorbance) in osteogenic cells derived from human alveolar bone fragments cultured on dense Ti and porous Ti**

Parameters	Time points (days)	Dense Ti (Mean ± SD)	Porous Ti (Mean ± SD)
Culture growth ($n = 4$)	3	0.11 ± 0.01	0.19 ± 0.01
	7	0.29 ± 0.02(b)	0.84 ± 0.13(a,b)
	10	0.43 ± 0.05(b)	0.88 ± 0.09(a,b)
Total protein content ($n = 4$)	7	22.18 ± 2.81	37.26 ± 1.76(a)
	10	58.51 ± 4.64(c)	83.69 ± 13.88(a,c)
ALP activity ($n = 4$)	7	46.90 ± 5.14	9.97 ± 3.70(a)
	10	34.75 ± 8.77(d)	9.68 ± 1.32(a)
Calcium content ($n = 5$)	17	2.39 ± 0.69	4.47 ± 0.77(a)

(a) Indicates statistically significant differences ($P \leq 0.05$) between Ti surfaces at each time point.
(b) Indicates statistically significant differences ($P \leq 0.05$) among 3 and 7 and 10 days.
(c) Indicates statistically significant difference ($P \leq 0.05$) between 7 and 10 days irrespective of Ti surface.
(d) Indicates statistically significant difference ($P \leq 0.05$) between 7 and 10 days to dense Ti.
SD, standard deviation.

cultures grew between 3 and 7 days ($P = 0.0147$ and 0.0002, respectively) and reached a plateau between 7 and 10 days ($P = 0.0898$ and 0.9675, respectively) (Fig. 3 and Table 2). Two-way ANOVA for the amount of total protein indicated significant differences regarding Ti surface ($P = 0.0001$), time ($P = 0.0001$), but not interaction Ti surface × time the ($P = 0.203$). The total protein content was greater on cultures grown on porous Ti and increased between 7 and 10 days (Fig. 4 and Table 2). For ALP activity, two-way ANOVA evidenced significant differences regarding Ti surface ($P = 0.0001$), time ($P = 0.043$), and Ti surface × time interaction ($P = 0.05$). ALP activity was higher on dense Ti at days 7 ($P = 0.002$) and 10 ($P = 0.0003$) (Fig. 5 and Table 2). For cultures grown on dense Ti, ALP activity decreased between 7 and 10 days ($P = 0.0363$) but not for porous Ti ($P = 0.9998$) (Fig. 5 and Table 2). The osteoblastic phenotype was confirmed at the transcriptional level by mRNA expression of the genes encoding Runx2, COL, ALP, BMP–7, and OC, in cultures grown on both dense Ti and porous Ti at days 7 and 17. For gene expression of Runx2, two-way ANOVA indicated significant differences regarding Ti surface ($P = 0.0001$), time ($P = 0.0001$), and Ti surface × time interaction ($P = 0.0001$). Gene expression of Runx2 on dense Ti was higher at day 7 ($P = 0.0002$) and lower at day 17 ($P = 0.0042$) (Fig. 6a and Table 3). Between 7 and 17 days, gene expression of Runx2 decreased in cultures grown on dense Ti ($P = 0.0002$), and did not change in cultures grown on porous Ti ($P = 0.1022$) (Fig. 6a and Table 3). Two-way ANOVA for gene expression of COL evidenced significant differences regarding Ti surface ($P = 0.0001$), time ($P = 0.0001$), and Ti surface × time interaction ($P = 0.0001$). For dense Ti, gene expression of COL was higher at day 7 ($P = 0.0002$) without significant difference from porous Ti at day 17 ($P = 0.4664$) (Fig. 6b and Table 3). Gene expression of COL decreased in cultures grown on dense Ti between 7 and 17 days ($P = 0.0002$) and did not change in cultures grown on porous Ti ($P = 0.4755$) (Fig. 6b and Table 3). For gene expression of ALP, two-way ANOVA showed a non-significant difference regarding Ti surface ($P = 0.131$) and significant differences in terms of time ($P = 0.0001$) and Ti surface × time interaction ($P = 0.0001$). Gene expression of ALP on dense Ti was higher at day 7 ($P = 0.0005$) and lower at day 17 ($P = 0.0002$) (Fig. 6c and Table 3). A decrease in gene expression of ALP was observed in cultures grown on dense Ti between 7 and 17 days ($P = 0.0375$) and an increase in cultures grown on porous Ti ($P = 0.0002$) (Fig. 6c and Table 3). For gene expression of BMP-7, two-way ANOVA indicated significant differences regarding Ti surface ($P = 0.029$), time ($P = 0.0001$),

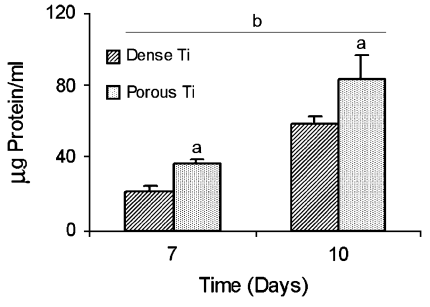

Fig. 4. Total protein content (µg/ml) of osteogenic cells derived from human alveolar bone cultured on dense titanium (Ti) and porous Ti for 7 and 10 days. (a) indicates statistically significant differences ($P \leq 0.05$) between Ti surfaces at each time point. (b) indicates statistically significant difference ($P \leq 0.05$) between 7 and 10 days irrespective of Ti surface. Data are reported as mean ± standard deviation ($n = 4$).

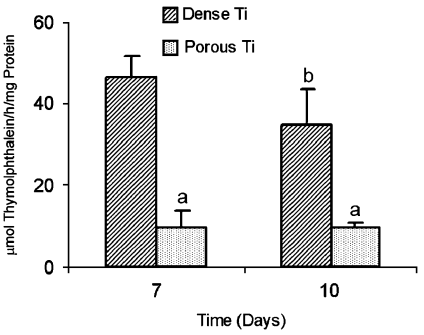

Fig. 5. Alkaline phosphatase (ALP) activity (µmol thymolphthalein/h/mg protein) of osteogenic cells derived from human alveolar bone cultured on dense titanium (Ti) and porous Ti for 7 and 10 days. (a) indicates statistically significant differences ($P \leq 0.05$) between Ti surfaces at each time point. (b) indicates statistically significant difference ($P \leq 0.05$) between 7 and 10 days to dense Ti. Data are reported as mean ± standard deviation ($n = 4$).

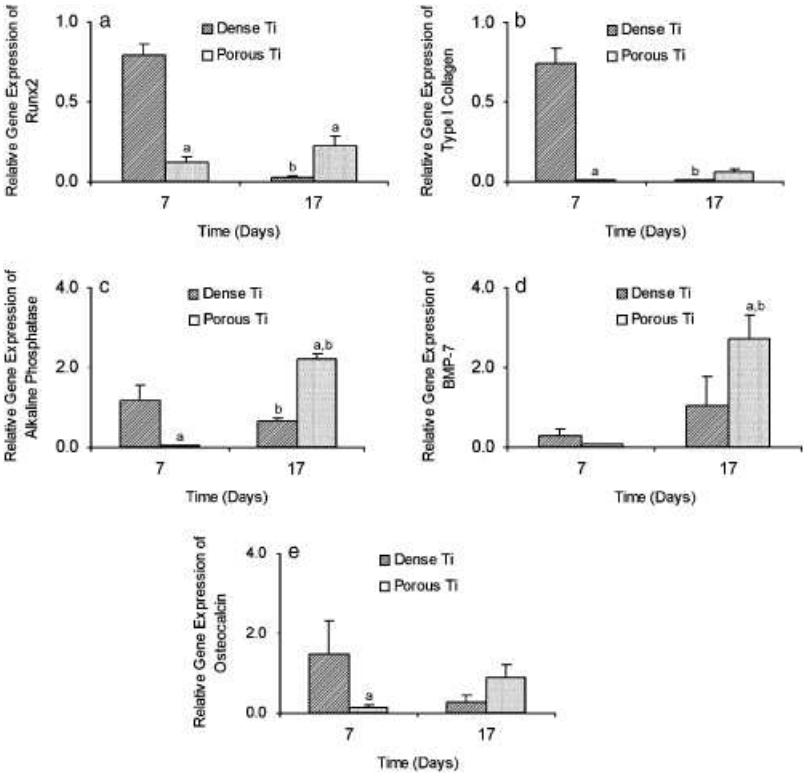

Fig. 6. Gene expression of runt-related transcription factor 2 (Runx2 – a), type I collagen (COL – b), alkaline phosphatase (ALP – c), bone morphogenetic protein–7 (BMP–7 – d), and osteocalcin (OC – e), in osteogenic cells derived from human alveolar bone cultured on dense titanium (Ti) and porous Ti for 7 and 17 days. (a) indicates statistically significant differences ($P \leq 0.05$) between Ti surfaces at each time point. (b) indicates statistically significant difference ($P \leq 0.05$) between 7 and 17 at each Ti surface. Data are reported as mean ± standard deviation ($n = 3$).

Table 3. **Gene expression of runt-related transcription factor 2 (Runx2), type I collagen (COL), alkaline phosphatase (ALP), bone morphogenetic protein–7 (BMP–7), and osteocalcin (OC) in osteogenic cells derived from human alveolar bone cultured on dense titanium (Ti) and porous Ti at days 7 and 17**

Gene	Time points (days)	Dense Ti (Mean ± SD)	Porous Ti (Mean ± SD)
Runx2	7	0.79 ± 0.07	0.12 ± 0.04(a)
	17	0.03 ± 0.01(b)	0.23 ± 0.06(a)
COL	7	0.75 ± 0.09	0.01 ± 0.00(a)
	17	0.01 ± 0.00(b)	0.06 ± 0.01
ALP	7	1.19 ± 0.36	0.02 ± 0.00(a)
	17	0.65 ± 0.06(b)	2.20 ± 0.14(a,b)
BMP–7	7	0.27 ± 0.19	0.05 ± 0.00
	17	1.03 ± 0.71	2.71 ± 0.61(a,b)
OC	7	1.47 ± 0.85	0.29 ± 0.17(a)
	17	0.13 ± 0.07	0.89 ± 0.30

(a) Indicates statistically significant differences ($P \leq 0.05$) between Ti surfaces at each time point.
(b) Indicates statistically significant difference ($P \leq 0.05$) between 7 and 17 at each Ti surface.
SD, standard deviation.

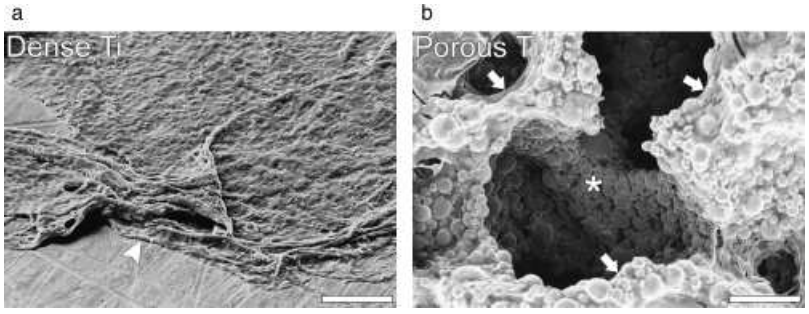

Fig. 7. High resolution scanning electron micrographs of osteogenic cells derived from human alveolar bone cultured on dense titanium (Ti) surface (a) and porous Ti structure (b) for 17 days. Areas of artificially-produced detachment (a, arrowhead) demonstrated that all surface of dense Ti was covered by a thin layer of tissue. On porous Ti structure, tissue ingrowth was restricted to the superficial regions (b, arrows) with absence of tissue in the deeper areas (b, asterisk). Scale bars: a = 50 μm; b = 200 μm.

and Ti surface × time interaction ($P = 0.009$). At 7 days, gene expression of BMP-7 was not affected by Ti surfaces ($P = 0.9422$) and was higher on porous Ti at day 17 ($P = 0.0112$) (Fig. 6d and Table 3). Gene expression of BMP-7 increased in cultures grown on porous Ti ($P = 0.0008$) between 7 and 17 days, and did not change in cultures grown on dense Ti ($P = 0.2777$) (Fig. 6d and Table 3). Two-way ANOVA for gene expression of OC demonstrated non-significant differences regarding Ti surface ($P = 0.199$) and time ($P = 0.452$) and a significant difference in the Ti surface × time interaction ($P = 0.006$). On dense Ti, gene expression of OC was higher at day 7 ($P = 0.03$) without a significant difference from porous Ti at day 17 ($P = 0.4364$) (Fig. 6e and Table 3). Gene expression of OC was not affected by the time in cultures grown on both dense Ti and porous Ti ($P = 0.0549$ and 0.2569, respectively) (Fig. 6e and Table 3). At 17 days, SEM micrographs revealed a layer of extracellular matrix coating the entire surface area of the dense Ti (Fig. 7a). Additionally, *in vitro* tissue ingrowth was restricted to the superficial regions of the porous Ti structure (Fig. 7b). The Alizarin Red S-stained cultures at day 17 exhibited areas of calcified matrix on both dense Ti and porous Ti (Fig. 8a and b). The calcium content measured by the extraction of Alizarin Red S from the mineralized matrix was significantly greater ($P = 0.009$) in cultures grown for 17 days on the porous Ti structure (Fig. 8c and Table 2).

Discussion

It is well established that surface properties of the biomaterials such as topography, chemistry, and surface energy direct cell–implant interactions (Puleo & Nanci 1999; Brunski et al. 2000; Bachle & Kohal 2004). Although Ti has been used as a successful and widespread implant material, a large number of studies have evaluated variations in the Ti surface properties. In this context, the present study aimed to investigate the human alveolar bone cell proliferation, expression of osteoblastic phenotype, and matrix mineralization on porous Ti produced by powder metallurgy and to make a comparison with dense Ti. The results showed that a porous Ti structure promotes the culture growth as indicated by MTT assay and total protein content, induces a delay in the acquisition of the osteoblastic phenotype as demonstrated by gene expression profile and ALP activity, and supports the enhancement of matrix mineralization.

It is widely accepted that the optimal pore size for the bone ingrowth is between 100 and 500 μm, and the pores must be interconnected to allow the organization of the vascular system required for continuing bone development (Bobyn et al. 1980; Ishaug-Riley et al. 1998; Li et al. 2005, 2007). Additionally, an average pore size ranging from 336 to 556 μm induced similar osteogenic cell responses to porous Ti fabricated using the same powder metallurgy process (St -Pierre et al. 2005). In accord with this, in this study we used discs of porous Ti with pore size varying between 50 and 400 μm. The high surface area of the porous Ti compared with the dense Ti is associated with the powder metallurgy process used (Lefebvre & Thomas 2003). Indeed, the starting material is a powder having a broad particle size distribution (-180 μm) and a high specific surface area (300 cm^2/g). During sintering at a high temperature under vacuum, thermal etching occurs and reveals the crystallographic planes of the Ti crystals (Gauthier et al. 2003). This provides the fine submicron-size steps and the high surface area exhibited by the porous Ti as demonstrated by SEM micrographs.

The cell source should not be neglected in studies of the interaction between cells and biomaterials as the development of the osteoblastic phenotype is skeletal site-specific, and is most probably related to different embryological origins and functions of each site (Akintoye et al. 2006). Alveolar bone is one of the most active bones in the human body and its osteoblastic cells are the ones that will interact with dental implant surfaces (Xiao et al. 2003). Because of this, in the present study, we

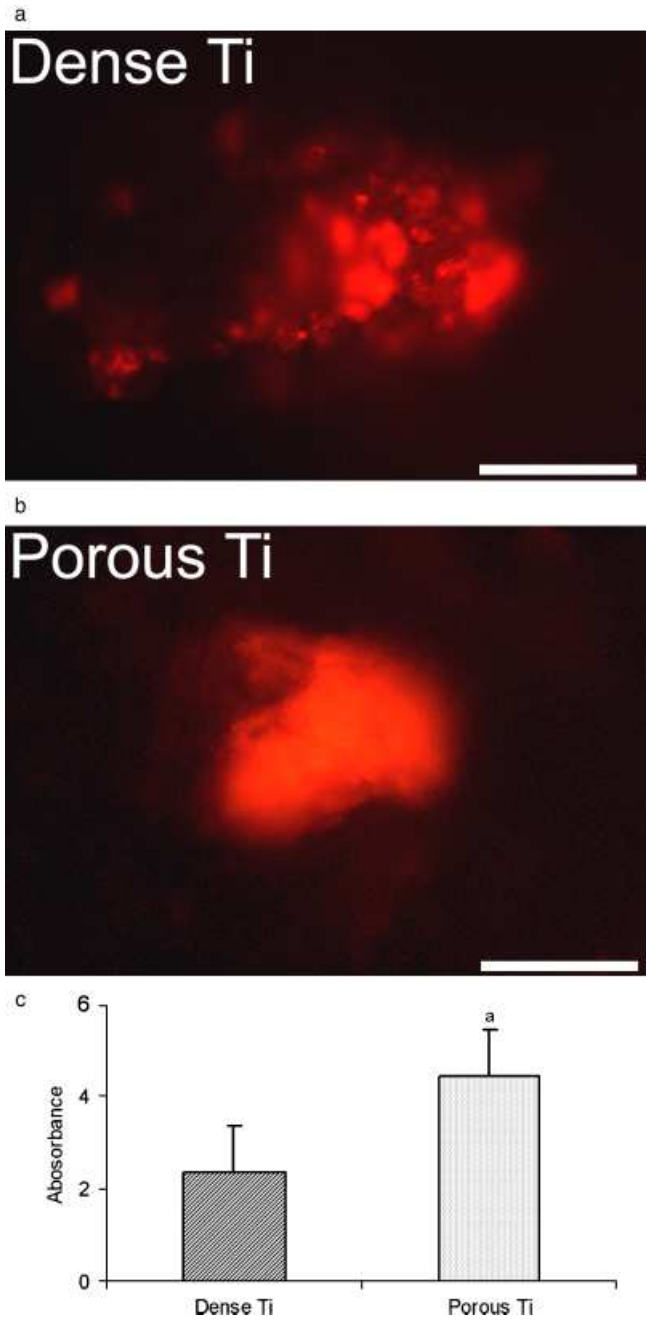

Fig. 8. Extracellular matrix mineralization at 17 days, stained with Alizarin red S for histochemical detection of calcium deposits. Epifluorescence of osteogenic cells derived from human alveolar bone cultured on dense titanium (Ti) (a) and porous Ti (b) with typical bone-like nodule formation. Calcium content (c; absorbance) extracted from mineralized matrix of osteogenic cultures grown on dense Ti and porous Ti. (a) indicates statistically significant difference ($P \leq 0.05$) between Ti surfaces. Data are reported as mean ± standard deviation ($n = 5$). Scale bars: a and b = 100 μm.

used osteoblastic cells derived from human alveolar bone fragments. In order for osteogenic cells to proceed with the wound-healing cascade – proliferation, differentiation, and tissue maturation – cells need to adhere and spread to a substrate first (Folkman & Moscona 1978; Burridge et al. 1987). In addition, changes in cell shape have been demonstrated to affect the fate of tissue growth (Chen et al. 1997; McBeath et al. 2004). In the present study, a dense Ti surface and a three-dimensional porous Ti structure supported different kinetics in cell spreading, as revealed by epifluorescence of actin cytoskeleton labelling. Indeed, cell spreading was clearly impaired on porous Ti possibly due to its surface geometry characteristics, with interconnecting spheres in the meso and micron-scale defining the limits for *in vitro* tissue ingrowth. Considering that the majority of adherent cells on both dense Ti and porous Ti were associated with extracellular fibronectin, the observed changes in cell morphology and in the pattern of fibronectin organization on porous Ti possibly affected initial cell–Ti interactions, altering the progression of the cultures and the expression of osteoblastic markers. Indeed, fibronectin has been demonstrated to be involved in the interactions between the implants and the extracellular matrix, acting on cell adhesion, spreading and differentiation, and matrix mineralization (Globus et al. 1998; Keselowsky et al. 2005; Luthen et al. 2005).

It has been shown that the architecture of the porous biomaterials may provide a favourable environment for cell growth. Cultures of osteoblasts derived from rat calvaria and human osteosarcoma cell line presented a higher proliferation rate on porous bioactive glass and porous hydroxyapatite, respectively, compared with dense surfaces (Anil Kumar et al. 2005; Valerio et al. 2005). Also, newborn mouse calvaria-derived MC3T3-E1 pre-osteoblastic cultures grown on porous Ti exhibited significantly more cells than on a dense Ti surface (St -Pierre et al. 2005). Corroborating these findings, in the present study, we noticeably demonstrated that parameters related to the culture growth such as reduction of MTT by the mitochondrial dehydrogenase of viable cells and total protein content were significantly increased in cultures of osteogenic cells grown on a porous Ti structure compared with dense Ti. In addition, these cells exhibited more synthetic activity as cell proliferation peaked between 7 and 10 days and the total protein content approximately increased two-fold from 7 to 10 days. The positive effect of porous biomaterials on cell proliferation could be attributed not only to the three-dimensional structure volume, which mimics the design of the trabecular bone and supports tissue ingrowth, but also to the large surface area available for cell growth (Holy et al. 2003; St-Pierre et al. 2005). However, although porous Ti exhibited a 225-fold larger area than that of dense Ti, cell growth was only

three-fold greater. This could be explained by the relatively reduced length of the culture period, as the inability of cells to penetrate into deeper regions was clearly noticed.

Significant differences have been demonstrated between dense Ti and porous Ti in terms of the development of the osteoblastic phenotype. For instance, a porous Ti structure induces a higher ALP activity compared with a dense Ti surface in MC3T3-E1 pre-osteoblastic cells cultured for periods of up to 13 days (St-Pierre et al. 2005). In contrast, our results demonstrated that osteogenic cells cultured on porous Ti exhibited a remarkably lower ALP activity at both time points evaluated: 7 and 10 days. Consistently, the expression of genes encoding Runx2, COL, ALP, BMP–7, and OC, key markers of the osteoblastic phenotype (Owen et al. 1990; Stein et al. 1990; Beck 2003), was delayed in cells cultured on porous Ti. Taken together, the results of cell growth and expression of the osteoblastic phenotype are supported by the reciprocal relationship between the decrease in cell proliferation and induction of differentiation (Owen et al. 1990).

Despite the reduced levels of ALP activity at days 7 and 10, such a three-dimensional Ti structure supported increased mineralized matrix formation at day 17, when mRNA of osteoblastic markers, including ALP, achieved higher levels compared with dense Ti. Interestingly, while the porous Ti structure supported an enlarged and more suitable environment for bone-like tissue formation, as also described by others (Kim et al. 2000; Holtorf et al. 2005; Li et al. 2007), dense Ti exhibited the majority of cells with typical changes in nuclear morphology indicative of apoptotic cell death at day 17, limiting the extension of mineralized matrix formation in such a reduced, two-dimensional environment. Therefore, the porous Ti structure extends the lifespan of osteogenic cells and possibly their synthetic activity phase, ultimately leading to an increase in bone tissue formation. However, the possibility that the greater surface area could account for the more *in vitro* tissue formation and therefore the enhancement in calcium deposits cannot be ruled out.

In conclusion, we have demonstrated that the porous Ti structure produced through a powder metallurgy process allowed human alveolar bone-derived cells to adhere, proliferate, and produce mineralized matrix. Additionally, porous Ti had a positive effect on the culture growth and the cell cycle activity, resulting in a delay in the expression of the osteoblastic phenotype. From our findings, strategies for developing novel biomaterials for implant application have raised. They include the association of the ability of porous Ti to induce tissue ingrowth with surface treatments that clearly demonstrate osteogenic potential, such as production of nanotopography or immobilization of selected molecules with known osteogenic activity (Nanci et al. 1998; Puleo et al. 2002; De Oliveira & Nanci 2004; De Oliveira et al. 2007). Finally, because *in vitro* tissue ingrowth may be restricted to the superficial regions of the porous Ti structure and a fully porous structure may exhibit reduced mechanical properties, porous-surfaced implants could be more suitable for implant applications (Li et al. 2005). Further studies are needed in order to determine the optimal thickness of the porous structure for cell/tissue ingrowth. Such strategies have been under investigation in our laboratory.

Acknowledgements: This work was supported by the National Council of Scientific and Technological Development (CNPq, Brazil), the State of Sao Paulo Research Foundation (FAPESP, Brazil), and the University of Sao Paulo (USP, Brazil). We would like to thank Fabíola S. de Oliveira, Roger R. Fernandes, and Júnia Ramos for the helpful assistance they provided during the cell culture experiments, Steven Lang from SIMS-NRC for the BET measurements and Eric Baril from IMI-NRC for the profilometry analysis.

References

Akintoye, S.O., Lam, T., Shi, S., Brahim, J., Collins, M.T. & Robey, P.G. (2006) Skeletal site-specific characterization of orofacial and iliac crest human bone marrow stromal cells in same individuals. *Bone* **38**: 758–768.

Anil Kumar, P.R., Varma, H.K. & Kumary, T.V. (2005) Rapid and complete cellularization of hydroxyapatite for bone tissue engineering. *Acta Biomaterialia* **1**: 545–552.

Assad, M., Jarzem, P., Leroux, M.A., Coillard, C., Chernyshov, A.V., Charette, S. & Rivard, C.H. (2003) Porous titanium-nickel for intervertebral fusion in a sheep model: part 1. Histomorphometric and radiological analysis. *Journal of Biomedical Materials Research B* **64**: 107–120.

Bachle, M. & Kohal, R.J. (2004) A systematic review of the influence of different titanium surfaces on proliferation, differentiation and protein synthesis of osteoblast-like MG63 cells. *Clinical Oral Implants Research* **15**: 683–692.

Beck, G.R. Jr (2003) Inorganic phosphate as a signaling molecule in osteoblast differentiation. *Journal of Cellular Biochemistry* **90**: 234–243.

Beloti, M.M., De Oliveira, P.T., Gimenes, R., Zaghete, M.A., Bertolini, M.J. & Rosa, A.L. (2006) In vitro biocompatibility of a novel membrane of the composite poly(vinylidene-trifluoroethylene)/barium titanate. *Journal of Biomedical Materials Research A* **79**: 282–288.

Beloti, M.M., Martins, W. Jr, Xavier, S.P. & Rosa, A.L. (2008) In vitro osteogenesis induced by cells derived from sites submitted to sinus grafting with an organic bovine bone. *Clinical Oral Implants Research* **19**: 48–54.

Bobyn, J.D., Pilliar, R.M., Cameron, H.U. & Weatherly, G.C. (1980) The optimum pore size for the fixation of porous-surfaced metal implants by the ingrowth of bone. *Clinical Orthopaedics and Related Research* **150**: 263–270.

Bobyn, J.D., Stackpool, G.J., Hacking, S.A., Tanzer, M. & Krygier, J.J. (1999) Characteristics of bone ingrowth and interface mechanics of a new porous tantalum biomaterial. *The Journal of Bone and Joint Surgery. (British Volume)* **81**: 907–914.

Brama, M., Rhodes, N., Hunt, J., Ricci, A., Teghil, R., Migliaccio, S., Rocca, C.D., Leccisotti, S., Lioi, A., Scandurra, M., De Maria, G., Ferro, D., Pu, F., Panzini, G., Politi, L. & Scandurra, R. (2007) Effect of titanium carbide coating on the osseointegration response in vitro and in vivo. *Biomaterials* **28**: 595–608.

Brånemark, P.I. (1983) Osseointegration and its experimental background. *The Journal of Prosthetic Dentistry* **50**: 399–410.

Brunski, J.B., Puleo, D.A. & Nanci, A. (2000) Biomaterials and biomechanics of oral and maxillofacial implants: current status and future developments. *The International Journal of Oral & Maxillofacial Implants* **15**: 15–46.

Burridge, K., Molony, L. & Kelly, L. (1987) Adhesion plaques: sites of transmembrane interaction between the extracellular matrix and the actin cytoskeleton. *Journal of Cell Science. Supplement* **8**: 211–229.

Castellani, R., de Ruijter, J.E., Renggli, H. & Jansen, J.A. (1999) Response of rat bone marrow cells to differently roughened titanium discs. *Clinical Oral Implants Research* **10**: 369–78.

Chen, C.S., Mrksich, M., Huang, S., Whitesides, G.M. & Ingber, D.E. (1997) Geometric control of cell life and death. *Science* **276**: 1425–1428.

De Oliveira, P.T. & Nanci, A. (2004) Nanotexturing of titanium-based surfaces upregulates expression of bone sialoprotein and osteopontin by cultured osteogenic cells. *Biomaterials* **25**: 403–413.

De Oliveira, P.T., Zalzal, S.F., Beloti, M.M., Rosa, A.L. & Nanci, A. (2007) Enhancement of in vitro osteogenesis on titanium by chemically produced nanotopography. *Journal of Biomedical Materials Research A* **80**: 554–564.

Faria, A.C., Beloti, M.M. & Rosa, A.L. (2003) Nitric acid passivation does not affect in vitro biocompatibility of titanium. *The International Journal of Oral & Maxillofacial Implants* **18**: 820–825.

Folkman, J. & Moscona, A. (1978) Role of cell shape in growth control. *Nature* **273**: 345–349.

Gauthier, M., Menini, R., Bureau, M.N., So, S.K.V., Dion, M.J. & Lefebvre, L.P. (2003) Properties of novel titanium foams intended for biomedical applications. ASM Materials and Processes for Medical Devices Conference, Anaheim, Californie, pp.382–387.

Globus, R.K., Doty, S.B., Lull, J.C., Holmuhamedov, E., Humphries, M.J. & Damsky, C.H. (1998) Fibronetin is a survival factor for differentiated osteoblasts. *Journal of Cell Science* **111**: 1385–1393.

Gregory, C.A., Gunn, W.G., Peister, A. & Prockop, D.J. (2004) An Alizarin red-based assay of mineralization by adherent cells in culture: comparison with cetylpyridinium chloride extraction. *Analytical Biochemistry* **329**: 77–84.

Holtorf, H.L., Datta, N., Jansen, J.A. & Mikos, A.G. (2005) Scaffold mesh size affects the osteoblastic differentiation of seeded marrow stromal cells cultured in a flow perfusion bioreactor. *Journal of Biomedical Materials Research A* **74**: 171–180.

Holy, C.E., Fialkov, J.A., Davies, J.E. & Shoichet, M.S. (2003) Use of a biomimetic strategy to engineer bone. *Journal of Biomedical Materials Research A* **15**: 447–453.

Ishaug-Riley, S.L., Crane-Kruger, G.M., Yaszemski, M.J. & Mikos, A.G. (1998) Three-dimensional culture of rat calvarial osteoblasts in porous biodegradable polymers. *Biomaterials* **19**: 1405–1412.

Keselowsky, B.G., Collard, D.M. & Garcia, A.J. (2005) Integrin binding specificity regulates biomaterial surface chemistry effects on cell differentiation. *Proceedings of the National Academy of Sciences of the United States of America* **102**: 5953–5957.

Kim, H.M., Kokubo, T., Fujibayashi, S., Nishiguchi, S. & Nakamura, T. (2000) Bioactive macroporous titanium surface layer on titanium substrate. *Journal of Biomedical Materials Research* **52**: 553–557.

Klokkevold, P.R., Nishimura, R.D., Adachi, M. & Caputo, A. (1997) Osseointegration enhanced by chemical etching of the titanium surface. *Clinical Oral Implants Research* **8**: 442–447.

Kroese-Deutman, H.C., van den Dolder, J., Spauwen, P.H. & Jansen, J.A. (2005) Influence of RGD-loaded titanium implants on bone formation in vivo. *Tissue Engineering* **11**: 1867–1875.

Lefebvre, L.P. & Baril, E. (2008) Effect of oxygen concentration and distribution on the compression properties on titanium foams. *Advanced Engineering Materials* **10**: 868–876.

Lefebvre, L.P. & Thomas, Y. (2003) Method of making open cell material. US Patent No. 6660224.

Li, J.P., Habibovic, P., van den Doel, M., Wilson, C.E., de Wijn, J.R., van Blitterswijk, C.A. & de Groot, K. (2007) Bone ingrowth in porous titanium implants produced by 3D fiber deposition. *Biomaterials* **28**: 2810–2820.

Li, J.P., Li, S.H., Van Blitterswijk, C.A. & de Groot, K. (2005) A novel porous Ti6Al4V: characterization and cell attachment. *Journal of Biomedical Materials Research A* **73**: 223–233.

Liu, X., Chu, P.K. & Ding, C. (2004) Surface modification of titanium, titanium alloys and related materials for biomedical applications. *Materials Science and Engineering: R: Reports* **47**: 49–121.

Livak, K.L. & Schmittgen, T.D. (2001) Analysis of relative gene expression data using real-time quantitative PCR and the 22DDCT method. *Methods* **25**: 402–408.

Lowry, O.H., Rosebrough, N.J., Farr, A.L. & Randall, R.J. (1951) Protein measurement with the Folin phenol reagent. *The Journal of Biologicla Chemistry* **193**: 265–275.

Luthen, F., Lange, R., Becker, P., Rychly, J., Beck, U. & Nebe, J.G. (2005) The influence of surface roughness of titanium on beta1- and beta3-integrin adhesion and the organization of fibronectin in human osteoblastic cells. *Biomaterials* **26**: 2423–2440.

Maniatopoulos, C., Pilliar, R.M. & Smith, D.C. (1986) Threaded versus porous surfaced designs for implant stabilization in bone-endodontic implant model. *Journal of Biomedical Materials Research* **20**: 1309–1333.

Maniatopoulos, C., Pilliar, R.M. & Smith, D.C. (1988a) Evaluation of shear strength at the cement-endodontic post interface. *The Journal of Prosthetic Dentistry* **59**: 662–669.

Maniatopoulos, C., Pilliar, R.M. & Smith, D.C. (1988b) Evaluation of the retention of endodontic implants. *The Journal of Prosthetic Dentistry* **59**: 438–446.

McBeath, R., Pirone, D.M., Nelson, C.M., Bhadriraju, K. & Chen, C.S. (2004) Cell shape, cytoskeletal tension, and RhoA regulate stem cell lineage commitment. *Developmental Cell* **6**: 483–495.

Melican, M.C., Zimmerman, M.C., Dhillon, M.S., Ponnambalam, A.R., Curodeau, A. & Parsons, J.R. (2001) Three-dimensional printing and porous metallic surfaces: a new orthopedic application. *Journal of Biomedical Materials Research* **55**: 194–202.

Mosmann, T. (1983) Rapid colorimetric assay for cellular growth and survival: application to proliferation and cytotoxicity assays. *Journal of Immunological Methods* **65**: 55–63.

Murray, G.A. & Semple, J.C. (1981) Transfer of tensile loads from a prosthesis to bone using porous titanium. *The Journal of Bone and Joint Surgery. (British Volume)* **63-B**: 138–141.

Nanci, A., Wuest, J.D., Peru, L., Brunet, P., Sharma, V., Zalzal, S. & McKee, M.D. (1998) Chemical modification of titanium surfaces for covalent attachment of biological molecules. *Journal of Biomedical Materials Research* **40**: 324–335.

Owen, T.A., Aronow, M., Shalhoub, V., Barone, L.M., Wilming, L., Tassinari, M.S., Kennedy, M.B., Pockwinse, S., Lian, J.B. & Stein, G.S. (1990) Progressive development of the rat osteoblast phenotype in vitro: reciprocal relationships in expression of genes associated with osteoblast proliferation and differentiation during formation of the bone extracellular matrix. *Journal of Cellular Physiology* **143**: 357–370.

Pilliar, R.M. (1983) Powder metal-made orthopedic implants with porous surface for fixation by tissue ingrowth. *Clinical Orthopaedics and Related Research* **176**: 42–51.

Pilliar, R.M. (1998) Overview of surface variability of metallic endosseous dental implants: textured and porous surface-structured designs. *Implant Dentistry* **7**: 305–314.

Pilliar, R.M., Cameron, H.U. & Macnab, I. (1975) Porous surface layered prosthetic devices. *Biomedical Engineering* **10**: 126–131.

Pilliar, R.M., Cameron, H.U., Welsh, R.P. & Binnington, A.G. (1981) Radiographic and morphologic studies of load-bearing porous-surfaced structured implants. *Clinical Orthopaedics and Related Research* **156**: 249–257.

Puleo, D.A., Kissling, R.A. & Sheu, M.S. (2002) A technique to immobilize bioactive proteins, including bone morphogenetic protein-4 (BMP-4), on titanium alloy. *Biomaterials* **23**: 2079–2087.

Puleo, D.A. & Nanci, A. (1999) Understanding and controlling the bone-implant interface. *Biomaterials* **20**: 2311–2321.

Rosa, A.L. & Beloti, M.M. (2003) Rat bone marrow cell response to titanium and titanium alloy with different surface roughness. *Clinical Oral Implants Research* **14**: 43–48.

Rosa, A.L., De Oliveira, C.S., Beloti, M.M., Xavier, S.P. & De Oliveira, P.T. (2006) Effect of microcapsules containing TAK-778 on bone formation around osseointegrated implants: histomorphometric analysis in dogs. *Implant Dentistry* **15**: 97–103.

Spiteri, C.G., Pilliar, R.M. & Kandel, R.A. (2006) Substrate porosity enhances chondrocyte attachment, spreading, and cartilage tissue formation in vitro. *Journal of Biomedical Materials Research A* **15**: 676–683.

Stein, G.S., Lian, J.B. & Owen, T.A. (1990) Relationship of cell growth to the regulation of tissue-specific gene expression during osteoblast differentiation. *The FASEB Journal* **4**: 3111–3123.

St -Pierre, P., Gauthier, M., Lefebvre, L.P. & Tabrizian, M. (2003) Human macrophage reaction to titanium foam processing residuals. Canadian Biomedical Society. Canadian Biomaterial Society Annual Meeting.

St -Pierre, J.P., Gauthier, M., Lefebvre, L.P. & Tabrizian, M. (2005) Three-dimensional growth of differentiating MC3T3-E1 pre-osteoblasts on porous titanium scaffolds. *Biomaterials* **26**: 7319–7328.

Valerio, P., Guimaraes, M.H., Pereira, M.M., Leite, M.F. & Goes, A.M. (2005) Primary osteoblast cell response to sol-gel derived bioactive glass foams. *Journal of Materials Science. Materials in Medicine* **16**: 851–856.

Wen, C.E., Yamada, K., Shimojima, K., Chino, Y., Asahina, T. & Mabuchi, M. (2002) Processing and mechanical properties of autogenous titanium implant materials. *Journal of Materials Science. Materials in Medicine* **13**: 397–401.

Xiao, Y., Qian, H., Young, W.G. & Bartold, P.M. (2003) Tissue engineering for bone regeneration using differentiated alveolar bone cells in collagen scaffolds. *Tissue Engineering* **9**: 1167–1177.